

# REV-ERB Agonism Improves Liver Pathology in a Mouse Model of NASH

Kristine Griffett\*, Gonzalo Bedia-Diaz, Bahaa El-Dien M. Elgendy, and Thomas P. Burris

Center for Clinical Pharmacology, Washington University School of Medicine and St. Louis College of Pharmacy, St. Louis, MO

\*Corresponding Author  
E-mail: [kgriffett@wustl.edu](mailto:kgriffett@wustl.edu)

## 26 **Abstract**

27 Non-alcoholic fatty liver disease (NAFLD) affects a significant number of people worldwide and  
28 currently there are no pharmacological treatments. NAFLD often presents with obesity, insulin  
29 resistance, and in some cases cardiovascular diseases. There is a clear need for treatment options to  
30 alleviate this disease since it often progresses to much more the much more severe non-alcoholic  
31 steatohepatitis (NASH). The REV-ERB nuclear receptor is a transcriptional repressor that regulates  
32 physiological processes involved in the development of NAFLD including lipogenesis and  
33 inflammation. We hypothesized that pharmacologically activating REV-ERB would suppress the  
34 progression of fatty liver in a mouse model of NASH. Using REV-ERB agonist SR9009 in a mouse  
35 NASH model, we demonstrate the beneficial effects of REV-ERB activation that led to an overall  
36 improvement of hepatic health by suppressing hepatic lipogenesis and inflammation.

## 37 **Introduction**

38 Among the metabolic disorders, non-alcoholic fatty liver disease (NAFLD) is considered a hepatic  
39 manifestation of metabolic syndrome (MetS) and it is one of the prominent health challenges of the  
40 twenty-first century as NAFLD is the most prevalent liver disease worldwide affecting 25-30% of the  
41 general population and its prevalence could reach 70-90% in specific populations with comorbidities  
42 such as morbid obesity or type 2 diabetes mellitus. NAFLD can often progress to non-alcoholic  
43 steatohepatitis (NASH), which is associated with progressive liver disease [1]. NASH has been  
44 mainly associated with higher morbidity and mortality than other diseases in the NAFLD spectrum  
45 and, although there are pharmacological therapies under clinical investigation for treatment of NASH  
46 [2], no drugs are approved by the Federal Drug Administration (FDA) or the European Medicines  
47 Agency (EMA) for the NASH treatment [3].

48 Nuclear receptors (NRs) are transcription factors generally activated by ligands and involved  
49 in diverse biological processes such as cell growth and differentiation, apoptosis, gene expression  
50 during tumor formation and metabolism. They bind to specific sequences of DNA allowing them to  
51 regulate the expression of adjacent genes. Many diseases including NASH are directly or indirectly  
52 related to nuclear receptor signaling and many NRs have become favored targets for drug discovery

53 [4]. NRs play an important role in liver diseases and they are key modulators in the onset and  
54 progression NAFLD, including the peroxisome proliferator-activated receptors (PPAR)  $\alpha/\beta/\gamma$ ; liver  
55 X receptors (LXR)  $\alpha/\beta$ ; farnesoid X receptors (FXR); constitutive androstane receptor (CAR); and  
56 pregnane X receptor (PXR). All of these NRs form obligate heterodimers with retinoid X receptor  
57 (RXR)  $\alpha/\beta/\gamma$  in order to modulate corresponding target genes in the nucleus. [5,6]

58 REV-ERB nuclear receptors (REV-ERB $\alpha$  and REV-ERB $\beta$ ) are transcriptional repressors  
59 that regulate a variety of physiological processes including lipogenesis, inflammation, circadian  
60 regulation, and muscle regeneration and are expressed in all tissues but has significantly higher  
61 expression in liver, skeletal muscle, adipose tissue, and brain [7]. Although REV-ERBs play a  
62 regulatory role in hepatic metabolism, inflammation and lipogenesis, these NRs have yet to be  
63 validated as a potential therapeutic target for liver disease [8–11]. Here, we show that REV-ERB  
64 agonist SR9009 treatment in *ob/ob* mice fed a high-fat, high-fructose (NASH) diet has beneficial  
65 effects and may provide some translational groundwork for further developing REV-ERB agonists  
66 for metabolic diseases, specifically NAFLD.

67

## 68 **Materials and Methods**

69

### 70 **Animals**

71 Animal studies were performed as previously described [12–14]. Briefly, six-week old B6 V-Lep<sup>ob</sup>/J  
72 (*ob/ob*) male mice were purchased from Jackson Labs (Bar Harbor, ME). Upon receipt, mice were  
73 housed individually in standard cages with huts and immediately placed on NASH diet (D09100301;  
74 Research Diets) [15]. Mice were maintained on this diet throughout the experiment. Mice were  
75 handled and weighed weekly while acclimating to the diet. At 12-weeks of age, mice were assigned  
76 into weight-matched groups (n = 6) and dosing began. Mice were weighed daily and food-intake was  
77 monitored daily. At the termination of the study, mice were euthanized by CO<sub>2</sub> and blood was  
78 collected by cardiac puncture for clinical chemistry (Roche COBAS) and ELISA analysis (EMD  
79 Millipore). Tissues were collected and flash-frozen in liquid nitrogen for gene expression, or placed  
80 in 4% Paraformaldehyde (PFA) in PBS for paraffin-embedding or 10% Neutral-Buffered Formalin

81 (NBF) for cryo-sectioning. All animal work was performed in accordance with the Institutional  
82 Animal Care and Use Committee (IACUC) at Washington University in St. Louis (Protocol  
83 #20180062).

84

### 85 **Compounds and Dosing**

86 SR9009 was formulated as 100mg/kg at 10mg/ml in 5% DMSO, 15% Cremophore EL (Sigma), 80%  
87 PBS as previously described [16]. Both vehicle (5% DMSO, 15% CremophoreEL (Sigma), 80% PBS)  
88 and SR9009 were filter sterilized (Millipore Steriflip) prior to dosing. Mice were given once daily  
89 i.p. injections within an hour of “lights on” (ZT0-ZT1). Dosing was performed for 30 days by the  
90 same researcher.

91

### 92 **Gene Expression Analysis**

93 Total RNA was isolated from liver using the trizol (Invitrogen) method [12]. Samples were analyzed  
94 by QPCR using Fatty Liver and Fibrosis QPCR array plates (Bio-Rad; 384-well format) and Bio-Rad  
95 supplied SYBR reagents (per manufacturer’s protocol). Each sample was run in duplicate and  
96 analyzed on the PrimePCR software supplied by Bio-Rad. Multiple reference genes were utilized  
97 (including Gapdh, ActinB, and Cyclophillin) for analysis [14]. Results were plotted in GraphPad  
98 prism software as Gene Regulation using mean +/- SEM.

99

### 100 **Tissue Lipid Analysis and Histology**

101 Livers for cryosectioning were incubated in 10% NBF at 4°C for 24-hours, then placed in 30%  
102 Sucrose in PBS at 4°C for cry-protection until the livers sank (approximately 2-6 days). Livers were  
103 then embedded in OCT freezing media in an ethanol-dry ice bath. Livers were cryo-sectioned at 10  
104 um thickness and floated in 12-well dishes in 1X PBS for Bodipy staining (10 sections per mouse).  
105 Sections were washed three times in cold 1X PBS and stained with Bodipy 493/503 per  
106 manufacturer’s protocol [12,14,17]. Livers that were placed in 4% PFA were paraffin-embedded and  
107 sectioned at 10 µm onto slides at the Saint Louis University Histology Core Facility. H&E and  
108 Masson’s Trichrome staining was performed at the core as a fee-for-service. Ten-sections per mouse

109 were slide scanned at the core facility and images were analyzed using ImageJ software (staining:total  
110 area) and plotted in GraphPad Prism [12,14,17].

111

## 112 **Statistics**

113 All data are expressed as mean +/- SEM (n = 4 or greater). All statistical analysis was performed  
114 using unpaired Student's t-test with Tukey's post-hoc analysis in GraphPad prism software.

115

## 116 **Results and Discussion**

117 Given that REV-ERBs have been demonstrated to play a regulatory role in hepatic lipid  
118 metabolism [18] as well as inflammation [16,18,19], we sought to examine the effects of  
119 pharmacologically activating REV-ERB in a mouse model of NASH and determine whether REV-  
120 ERB may be a therapeutically relevant target. We opted to utilize a diet-induced NASH model using  
121 *ob/ob* mice as previously described [14,15] as the time period for development of NAFLD with  
122 fibrosis (NASH) is relatively short as compared to other models. During the acclimation and NASH  
123 development period, mice were fed a diet that contains Primex as a trans-fat source, fructose, and  
124 cholesterol *ad libitum* and monitored for weight gain and food intake. These parameters were also  
125 monitored daily throughout the dosing period to validate that any weight-loss was not due to loss of  
126 appetite. As shown in Figure 1A, both groups (Vehicle and SR9009) gained weight throughout the  
127 experimental period, however the SR9009-treated group gained weight at a consistently slower rate.  
128 The slower weight gain was not due to lower food intake in the SR9009-treated mice since this group  
129 consistently consumed the same amount of food as the vehicle group (Figure 1B). After 30-days of  
130 dosing was completed, mice were euthanized, and we performed a variety of tissue and plasma  
131 analyses to determine whether SR9009 treatment had a beneficial effect in this model. While we did  
132 not see a significant effect in overall liver weight (Figure 1C), we did observe a significant decrease  
133 in blood-glucose levels in the SR9009-treated mice. The *ob/ob* mouse model is typically  
134 hyperglycemic and addition of the high fat/high fructose diet hyperglycemia can be particularly  
135 prominent. Thus, our observation that of lowered hyperglycemia was promising and potentially

136 relevant to human NASH patients who often present with co-morbidities such as obesity and diabetes  
137 [20–24].

138  
139 **Figure 1: REV-ERB agonist treatment of ob/ob NASH diet-fed mice.**

140 Mouse weight (A) and food intake (B) were recorded daily and averaged weekly for each group. At  
141 the termination of the experiment, mice were euthanized and blood and tissues were collected for  
142 analysis. Panel C shows the average liver weight as a percentage of the total body weight for each  
143 group. Blood glucose (D), ALT (E), AST (F), circulating triglycerides (G), and total protein (H) were  
144 also analyzed from blood plasma.

145  
146 We were interested in determining whether SR9009 had any utility in improving the hepatic  
147 health of these mice. In order to make this determination, we performed clinical chemistry analysis  
148 on blood plasma samples to examine liver enzyme levels (ALT and AST) (Figures 1E and 1F  
149 respectively), as well as circulating triglyceride levels (Figure 1G) and total protein levels (Figure  
150 1H) in both mouse groups. Plasma levels of liver enzymes are typically elevated in NASH due to  
151 liver damage and we observed that ALT levels were significantly reduced in the SR9009-treated mice  
152 (Figure 1E). These data clearly suggest that that the amount of liver damage due to the diet may be  
153 suppressed by treatment with REV-ERB agonist SR9009. While not statistically significant, AST  
154 levels in the SR9009 group were also trending lower than the vehicle group consistent with a benefit  
155 due to SR9009 treatment. We also observed significantly reduced circulating triglycerides as well as  
156 total protein in the plasma of SR9009 mice as compared to vehicle-treated mice. Our overall  
157 impression from the clinical chemistry data and mouse observations is that SR9009 treatment may  
158 have beneficial effects in a NASH model.

159 As the SR9009 group maintained a lower body weight throughout the dosing period and had  
160 significantly decreased circulating lipid levels in blood plasma, we investigated whether the SR9009-  
161 treated mice had reduced hepatosteatosis by staining for neutral lipids with Bodipy 493/503  
162 [12,14,17]. Figure 2A shows representative results of the Bodipy staining (green) in vehicle and  
163 SR9009-treated liver sections, which suggests that there are fewer lipid droplets in the SR9009 group.  
164 The Bodipy staining was quantified using ImageJ software and normalized to total area, plotted as  
165 relative fluorescence units (RFU) in Figure 2B. There was a significant decrease in lipid staining in

166 the SR9009-treated group, suggesting that SR9009 treatment suppressed circulating lipids (Figure  
167 1G), it was also suppressed the storage/accumulation of triglycerides in the livers of the treated  
168 animals.

169  
170 **Figure 2: SR9009 reduces hepatosteatosis in ob/ob mice maintained on a NASH diet.**

171 Bodipy 493/503 staining (green) for neutral lipids in 10  $\mu$ m liver cryosections counterstained with  
172 DAPI (blue) in vehicle- and SR9009-treated mice. Quantification of Bodipy staining was performed  
173 using ImageJ and demonstrates that the amount of lipids is significantly decreased in SR9009 mice  
174 as compared to vehicle.

175  
176 To validate the clinical chemistry data suggesting that the SR9009 reduced liver damage and  
177 the Bodipy data suggesting that SR9009 treatment decreased hepatosteatosis, we performed  
178 hematoxylin and eosin (H&E) staining on paraffin-embedded liver tissue and examined liver  
179 morphology (Figure 3). The top panels are 10X imaging of representative vehicle (left) and SR9009-  
180 treated (right) liver sections. While both groups display some level of steatosis, it is clear that the  
181 SR9009 group displayed reduced macrosteatosis and improved tissue morphology. The 20X (bottom)  
182 panels clearly illustrate that both macrosteatosis and microsteatosis are reduced in SR9009 tissue.  
183 H&E staining also indicated severe disease in vehicle sections, with an increase in the number of  
184 inflammatory foci and hepatocellular ballooning, in addition to increased steatosis, which is  
185 indicative of a NASH phenotype while the SR9009 group did not appear to progress further than a  
186 simple fatty liver phenotype.

187  
188 **Figure 3: H&E stained paraffin-embedded liver sections illustrating improved tissue**  
189 **morphology in SR9009-treated mice.**

190 Top panels (10X); Bottom panels (20X). Blue arrows indicate macrosteatosis; Yellow arrows indicate  
191 microsteatosis; orange arrows indicate inflammatory foci; and green arrows indicate hepatic  
192 ballooning.

193  
194 To continue our investigation into whether pharmacological activation of REV-ERB is  
195 beneficial in an NASH model, we analyzed gene expression of inflammatory markers by QPCR from  
196 frozen mouse liver tissues. For this analysis, we focused on expression changes related to  
197 inflammatory markers that indicate progression of NAFLD towards a NASH pathology. Previous  
198 work from our lab [16] and others have shown that REV-ERBs regulate a variety of genes involved

199 in the pathogenesis of metabolic diseases including those associated with inflammation. Specifically,  
200 we were interested to see whether we were suppressing the progression of NAFLD towards NASH  
201 with SR9009 by not only alleviating liver damage as assessed in Figure 1E-H, but by also suppressing  
202 hepatic inflammation in these animals, which was suggested in the H&E staining (Figure 3). Indeed,  
203 when compared to the vehicle-treated group, the SR9009 mice display significantly lower levels of  
204 expression of inflammatory cytokines including *IL-1a*, *IL-1b*, *TNFa*, and *Interferon gamma (IFNg)*,  
205 all of which have been implicated as biomarkers in NASH (Figure 4A).

206  
207 **Figure 4: Expression of inflammatory markers are downregulated by SR9009 treatment in a**  
208 **mouse model of NASH.**

209 (A) Gene expression of inflammatory cytokines in mouse liver tissues that are involved in the  
210 pathogenesis of NAFLD-NASH. (B) Masson-Trichrome staining of Vehicle-treated and SR9009-  
211 treated mouse liver paraffin-embedded sections (10um). Blue staining indicates collagen, suggesting  
212 that hepatic fibrosis is present. (C) Collagen staining was quantified using ImageJ software and  
213 suggests that SR9009 treatment suppressed the development of fibrosis in these samples. (D) An  
214 ELISA for mouse TNF $\alpha$  was performed using plasma samples from each mouse in triplicate and  
215 shows that SR9009 mice had significantly reduced circulating TNF $\alpha$ . (E) Gene expression was  
216 performed for *Col3A1* and *Stat1* genes, both of which are involved in the development of fibrosis in  
217 NAFLD/NASH. As shown in the graphs, both genes are significantly downregulated in SR9009 mice.

218  
219 Progression of NAFLD to NASH is associated with hepatic fibrosis, and in order to determine  
220 the level of fibrosis in this model we stained paraffin-embedded liver sections with Masson's  
221 trichrome (Figure 4B). Similar to the H&E stained liver sections, hepatic tissue from SR9009-treated  
222 mice display a more "normal" appearance with less macrosteatosis. The hallmark of this staining  
223 technique is the bright blue stain indicative of collagen fibers, which we quantitated as shown in  
224 Figure 4B. The livers from vehicle-treated mice appeared to have significantly increased blue  
225 staining, suggesting the progression of the disease towards a NASH phenotype with collagen deposits  
226 and fibrosis. While there is some indication of collagen deposits in the 20X image of the SR9009  
227 group, when quantified, there is a significant decrease in collagen staining suggesting that SR9009  
228 treatment inhibited fibrosis in these mice (Figure 4C). To further characterize the effects of SR9009  
229 on inflammation, we also assessed plasma TNF $\alpha$  levels. High levels of TNF $\alpha$  are associated with  
230 increased hepatic inflammation and poorer prognosis in NASH patients. As shown in Figure 4D, the  
231 SR9009-treated group had significantly lower plasma TNF $\alpha$  levels, which is in agreement with the



232 hepatic gene expression data (Figure 4A). Additionally, we assessed the level of expression of  
233 additional genes specifically involved in the development of hepatic fibrosis. *Collagen 3A1* gene  
234 (*COL3A1*) and *STAT1* are both considered biomarkers of NASH development and progression [25].  
235 In our experiments, both of these genes were significantly down regulated in SR9009-treated mice  
236 (Figure 4E), indicating that pharmacological activation of REV-ERB may dampen the progression of  
237 NAFLD towards NASH by not only suppressing hepatic lipid storage/accumulation, but also  
238 suppressing the activation of pro-inflammatory cytokines that are involved in the development of  
239 hepatic fibrosis.

240 Over the last several years, many studies by our lab and others have demonstrated that the  
241 REV-ERBs regulate a variety of genes involved in lipogenesis, metabolism, and inflammation.  
242 Several studies have investigated potential of REV-ERB agonists as potential therapeutics for cardio-  
243 metabolic diseases including atherosclerosis which is a common comorbidity with NAFLD or NASH  
244 [16,19]. Understanding the critical role that the REV-ERBs play in these pathways, we hypothesized  
245 that pharmacological activation of REV-ERB with the tool compound SR9009 in a mouse model of  
246 NASH would provide beneficial metabolic effects in the liver leading to reduced NASH pathology.  
247 Our data suggests that not only did SR9009 improve hepatic morphology by reducing hepatosteatosis,  
248 it also suppressed the activation of pro-inflammatory cytokines that are essential for the progression  
249 of NAFLD to NASH. While the SR9009 group did not gain weight at the same rate as the vehicle  
250 group and we cannot validate whether this was a direct effect of the compound, although feeding and  
251 other behaviors were observed to be the same for both groups throughout the study. In summary, our  
252 data suggests that REV-ERB is a potential therapeutic target to treat NASH. The REV-ERB agonist  
253 SR9009 displayed efficacy in reduction of hepatic pathology associated with NASH. SR9009 is  
254 effective in suppressing clinical markers of liver damage, circulating lipids, hepatic fibrosis and  
255 markers of inflammation. Our data suggests that REV-ERB agonists may offer novel therapies for  
256 NAFLD or NASH.

257

## 258 **Acknowledgments**

259 Barb Nagel at Saint Louis University School of Medicine (St. Louis, MO) Histology Core for paraffin  
260 embedding and performing histological staining of liver sections. Melissa Kazantzis at The Scripps  
261 Research Institute in Jupiter, FL for performing clinical chemistry analysis on samples. Sherry Burris  
262 for performing the cryopreservation and cryo-sectioning of liver samples for Bodipy analysis.

263

## 264 **References**

- 265 1. Fazel Y, B. Koenig A, Sayiner M, D. Goodman Z, M. Younossi Z. Epidemiology and natural  
266 history of non-alcoholic fatty liver disease [Internet]. *Metabolism*. 2016. pp. 1017 – 1025.  
267 doi:<https://doi.org/10.1016/j.metabol.2016.01.012>
- 268 2. Polyzos SA, Kang ES, Boutari C, Rhee E-J, Mantzoros CS. Current and emerging  
269 pharmacological options for the treatment of nonalcoholic steatohepatitis. *Metabolism*.  
270 Elsevier BV; 2020; 154203. doi:10.1016/j.metabol.2020.154203
- 271 3. Konerman MA, Jones JC, Harrison SA. Pharmacotherapy for NASH: Current and emerging.  
272 *Journal of Hepatology*. Elsevier BV; 2018;68: 362–375. doi:10.1016/j.jhep.2017.10.015
- 273 4. Yang X, Gonzalez FJ, Huang M, Bi H. Nuclear receptors and non-alcoholic fatty liver disease:  
274 An update. *Liver Research*. Elsevier BV; 2020; doi:10.1016/j.livres.2020.03.001
- 275 5. Tanaka N, Aoyama T, Kimura S, Gonzalez FJ. Targeting nuclear receptors for the treatment  
276 of fatty liver disease. *Pharmacology & Therapeutics*. Elsevier BV; 2017;179: 142–157.  
277 doi:10.1016/j.pharmthera.2017.05.011
- 278 6. López-Velázquez JA, Carrillo-Córdova LD, Chávez-Tapia NC, Uribe M, Méndez-Sánchez  
279 N. Nuclear Receptors in Nonalcoholic Fatty Liver Disease. *Journal of Lipids*. Hindawi  
280 Limited; 2012;2012: 1–10. doi:10.1155/2012/139875
- 281 7. Preitner N, Damiola F, Luis-Lopez-Molina, Zakany J, Duboule D, Albrecht U, et al. The  
282 Orphan Nuclear Receptor REV-ERB $\alpha$  Controls Circadian Transcription within the Positive  
283 Limb of the Mammalian Circadian Oscillator. *Cell*. Elsevier BV; 2002;110: 251–260.  
284 doi:10.1016/s0092-8674(02)00825-5
- 285 8. Li T, Eheim AL, Klein S, Uschner FE, Smith AC, Brandon-Warner E, et al. Novel role of  
286 nuclear receptor rev-erb $\alpha$  in hepatic stellate cell activation: Potential therapeutic target for  
287 liver injury. *Hepatology*. Wiley; 2014;59: 2383–2396. doi:10.1002/hep.27049
- 288 9. Stujanna EN, Murakoshi N, Tajiri K, Xu D, Kimura T, Qin R, et al. Rev-erb agonist improves  
289 adverse cardiac remodeling and survival in myocardial infarction through an anti-  
290 inflammatory mechanism. Fan G-C, editor. *PLOS ONE*. Public Library of Science (PLoS);  
291 2017;12: e0189330. doi:10.1371/journal.pone.0189330
- 292 10. Kojetin D.J. and Burris T.P. A Role for Rev-erb $\alpha$  Ligands in the Regulation of Adipogenesis.  
293 *Current Pharmaceutical Design*. Bentham Science Publishers Ltd.; 2011;17: 320–324.  
294 doi:10.2174/138161211795164211
- 295
- 296
- 297
- 298
- 299
- 300
- 301
- 302
- 303
- 304

- 305 11. Pariollaud M, Gibbs JE, Hopwood TW, Brown S, Begley N, Vonslow R, et al. Circadian clock  
306 component REV-ERB $\alpha$  controls homeostatic regulation of pulmonary inflammation. *Journal*  
307 *of Clinical Investigation*. American Society for Clinical Investigation; 2018;128: 2281–2296.  
308 doi:10.1172/jci93910  
309
- 310 12. Griffett K, Solt LA, El-Gendy BE-DM, Kamenecka TM, Burriss TP. A Liver-Selective LXR  
311 Inverse Agonist That Suppresses Hepatic Steatosis. *ACS Chemical Biology*. American  
312 Chemical Society (ACS); 2012;8: 559–567. doi:10.1021/cb300541g  
313
- 314 13. Griffett K, Burriss TP. Promiscuous activity of the LXR antagonist GSK2033 in a mouse  
315 model of fatty liver disease. *Biochemical and Biophysical Research Communications*.  
316 Elsevier BV; 2016;479: 424–428. doi:10.1016/j.bbrc.2016.09.036  
317
- 318 14. Griffett K, Welch RD, Flaveny CA, Kolar GR, Neuschwander-Tetri BA, Burriss TP. The LXR  
319 inverse agonist SR9238 suppresses fibrosis in a model of non-alcoholic steatohepatitis.  
320 *Molecular Metabolism*. Elsevier BV; 2015;4: 353–357. doi:10.1016/j.molmet.2015.01.009  
321
- 322 15. Trevaskis JL, Griffin PS, Wittmer C, Neuschwander-Tetri BA, Brunt EM, Dolman CS, et al.  
323 Glucagon-like peptide-1 receptor agonism improves metabolic, biochemical, and  
324 histopathological indices of nonalcoholic steatohepatitis in mice [Internet]. *American Journal*  
325 *of Physiology-Gastrointestinal and Liver Physiology*. 2012. pp. G762–G772.  
326 doi:10.1152/ajpgi.00476.2011  
327
- 328 16. Sitaula S, Billon C, Kamenecka TM, Solt LA, Burriss TP. Suppression of atherosclerosis by  
329 synthetic REV-ERB agonist. *Biochemical and Biophysical Research Communications*.  
330 Elsevier BV; 2015;460: 566–571. doi:10.1016/j.bbrc.2015.03.070  
331
- 332 17. Sengupta M, Griffett K, Flaveny CA, Burriss TP. Inhibition of Hepatotoxicity by a LXR  
333 Inverse Agonist in a Model of Alcoholic Liver Disease. *ACS Pharmacology & Translational*  
334 *Science*. American Chemical Society (ACS); 2018;1: 50–60. doi:10.1021/acsptsci.8b00003  
335
- 336 18. Solt LA, Wang Y, Banerjee S, Hughes T, Kojetin DJ, Lundasen T, et al. Regulation of  
337 circadian behaviour and metabolism by synthetic REV-ERB agonists. *Nature*. Springer  
338 Science and Business Media LLC; 2012;485: 62–68. doi:10.1038/nature11030  
339
- 340 19. Pourcet B, Zecchin M, Ferri L, Beauchamp J, Sitaula S, Billon C, et al. Nuclear Receptor  
341 Subfamily 1 Group D Member 1 Regulates Circadian Activity of NLRP3 Inflammasome to  
342 Reduce the Severity of Fulminant Hepatitis in Mice. *Gastroenterology*. Elsevier BV;  
343 2018;154: 1449–1464.e20. doi:10.1053/j.gastro.2017.12.019  
344
- 345 20. Petit J-M, Vergès B. GLP-1 receptor agonists in NAFLD. *Diabetes & Metabolism*. Elsevier  
346 BV; 2017;43: 2S28–2S33. doi:10.1016/s1262-3636(17)30070-8  
347
- 348 21. Scorletti E, Byrne CD. Extrahepatic Diseases and NAFLD: The Triangular Relationship  
349 between NAFLD, Type 2-Diabetes and Dysbiosis. *Digestive Diseases*. S. Karger AG;  
350 2016;34: 11–18. doi:10.1159/000447276  
351
- 352 22. Obesity, Type 2 diabetes and NAFLD. *Diabetic Medicine*. Wiley; 2014;31: 1–3.  
353 doi:10.1111/dme.12377\_1  
354

- 355 23. Portillo-Sanchez P, Cusi K. Treatment of Nonalcoholic Fatty Liver Disease (NAFLD) in  
356 patients with Type 2 Diabetes Mellitus. *Clinical Diabetes and Endocrinology*. Springer  
357 Science and Business Media LLC; 2016;2. doi:10.1186/s40842-016-0027-7  
358
- 359 24. Bonora E. Novel predictors of diabetes - NAFLD, diabetes and CVD. *Endocrine Abstracts*.  
360 *Bioscientifica*; 2017; doi:10.1530/endoabs.49.s29.3  
361
- 362 25. Feng G, Li X-P, Niu C-Y, Liu M-L, Yan Q, Fan L-P, et al. Bioinformatics analysis reveals  
363 novel core genes associated with nonalcoholic fatty liver disease and nonalcoholic  
364 steatohepatitis [Internet]. *Gene*. 2020. p. 144549.  
365 doi:<https://doi.org/10.1016/j.gene.2020.144549>

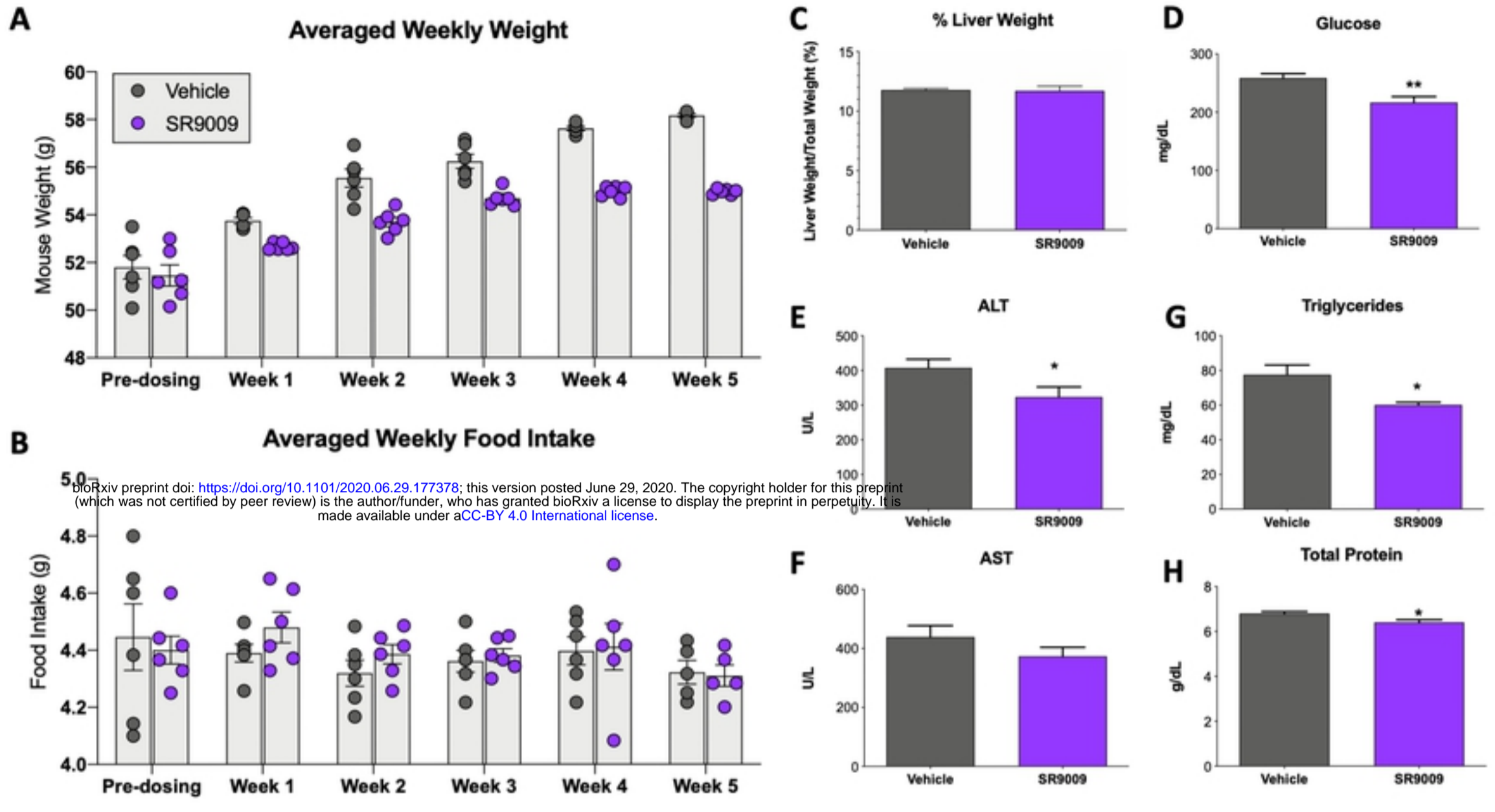


Figure 1

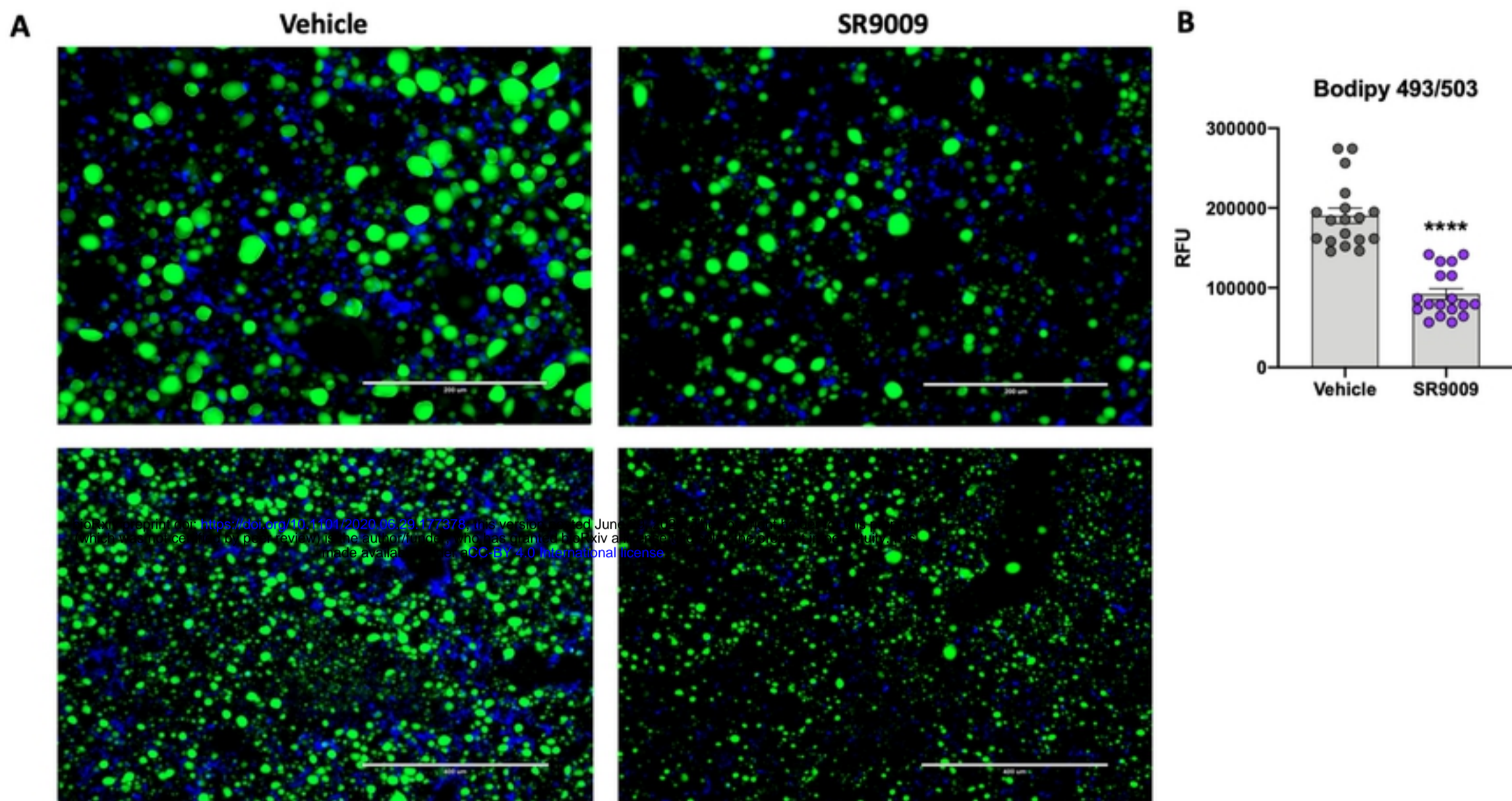
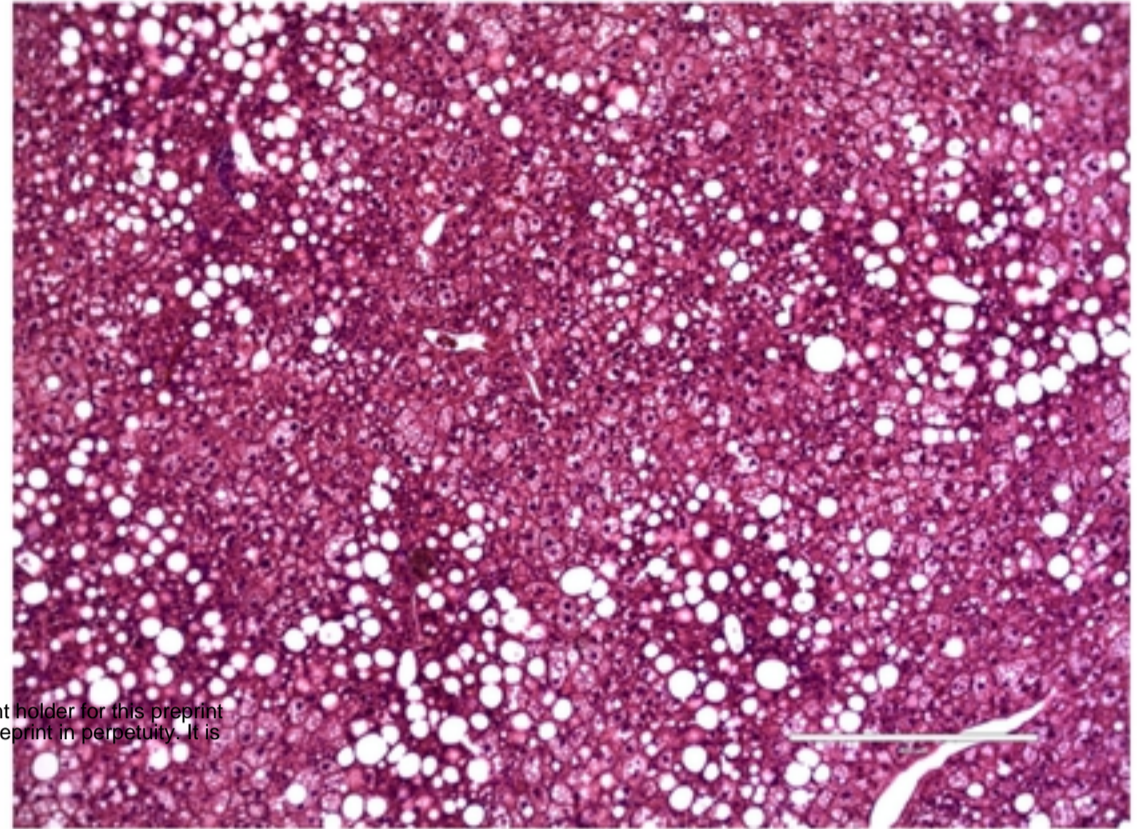
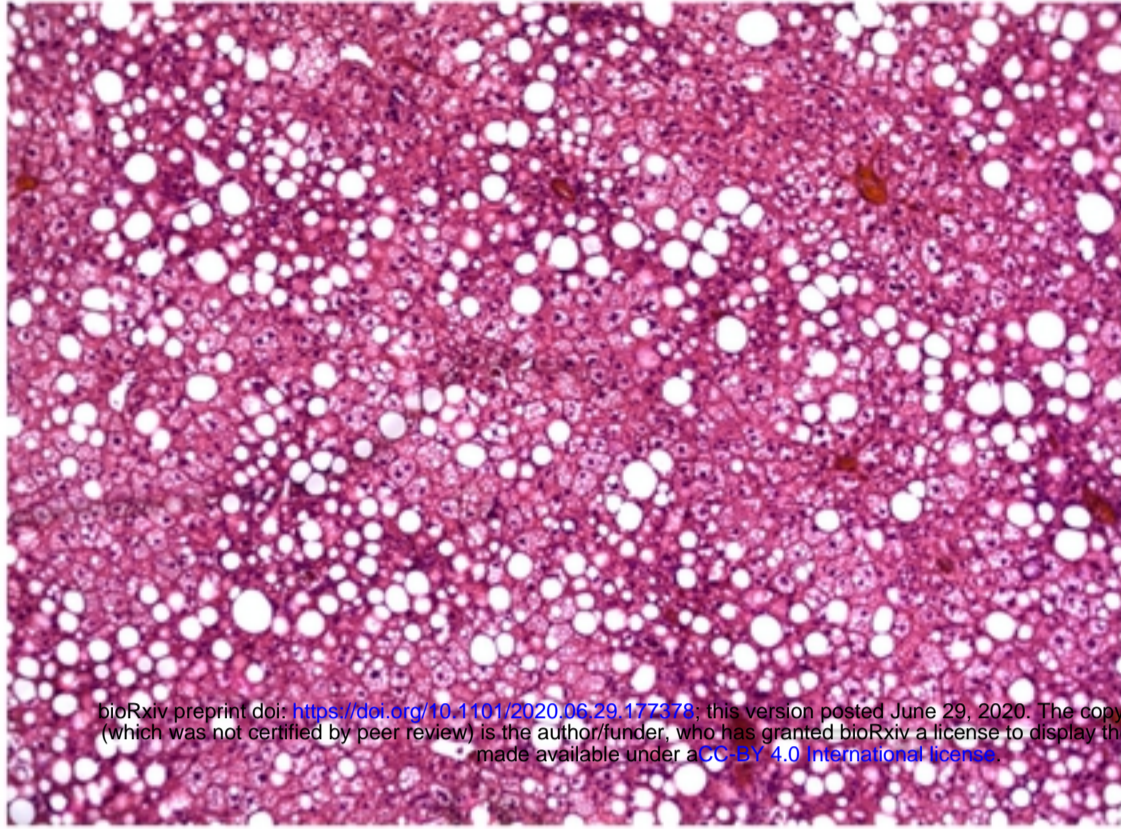


Figure 2

**Vehicle**

**SR9009**



bioRxiv preprint doi: <https://doi.org/10.1101/2020.06.29.177378>; this version posted June 29, 2020. The copyright holder for this preprint (which was not certified by peer review) is the author/funder, who has granted bioRxiv a license to display the preprint in perpetuity. It is made available under aCC-BY 4.0 International license.

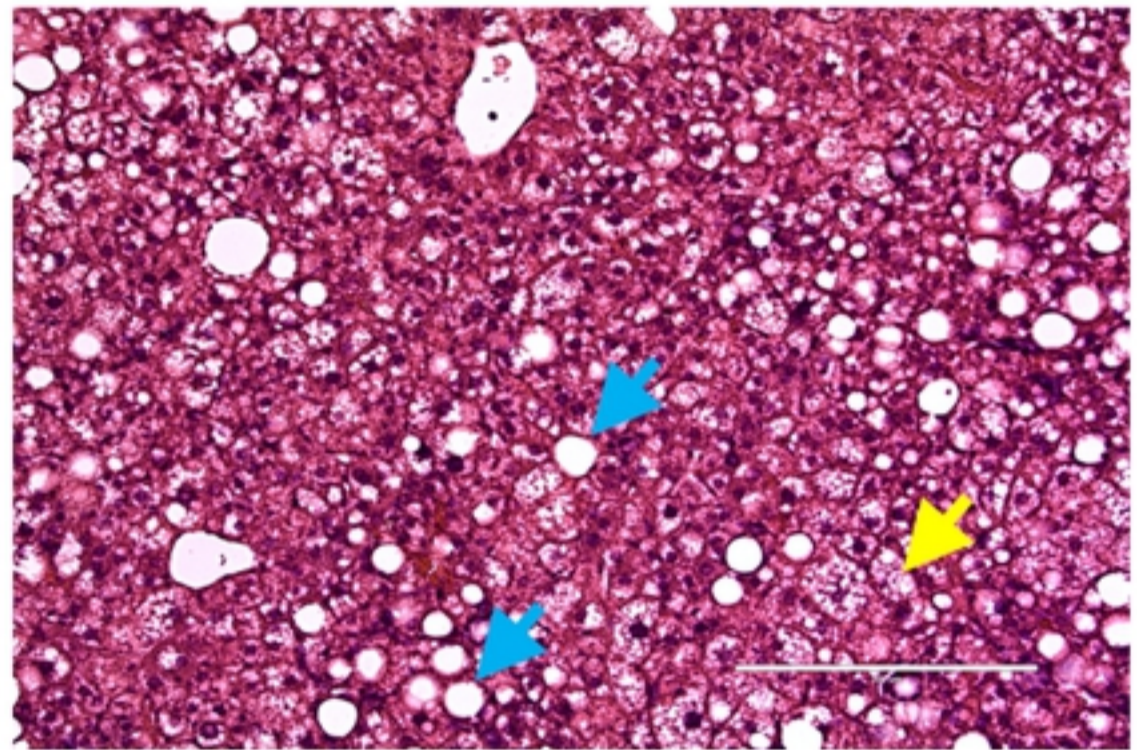
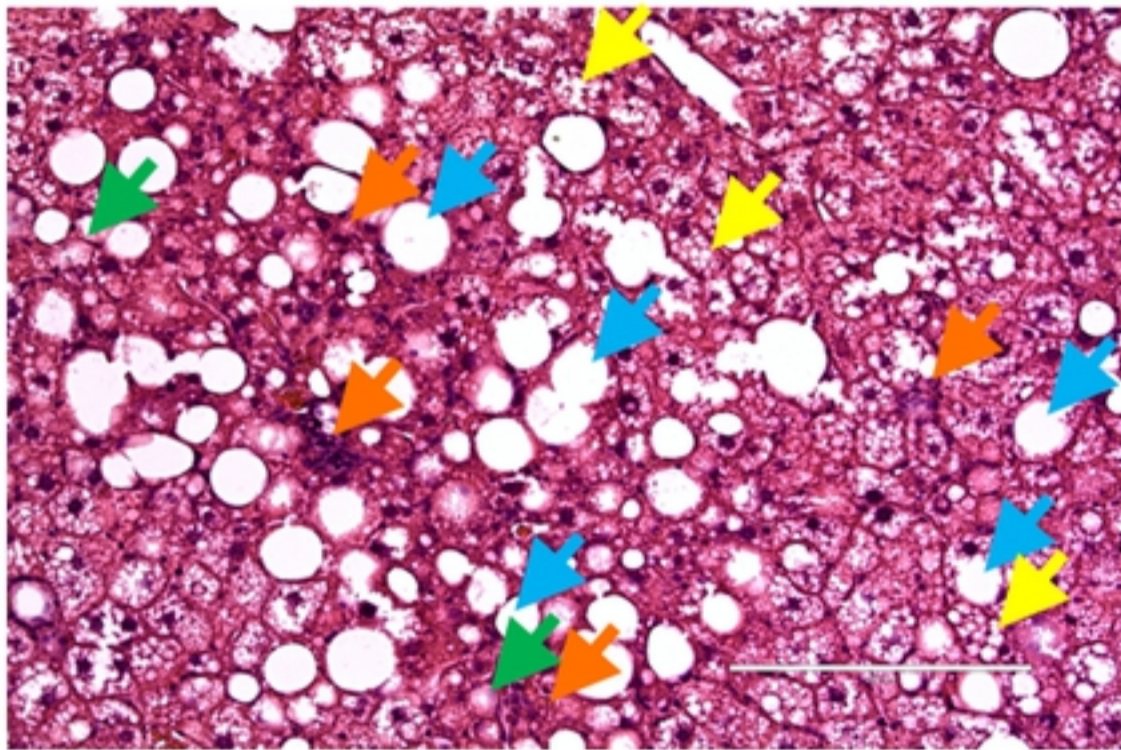


Figure 3

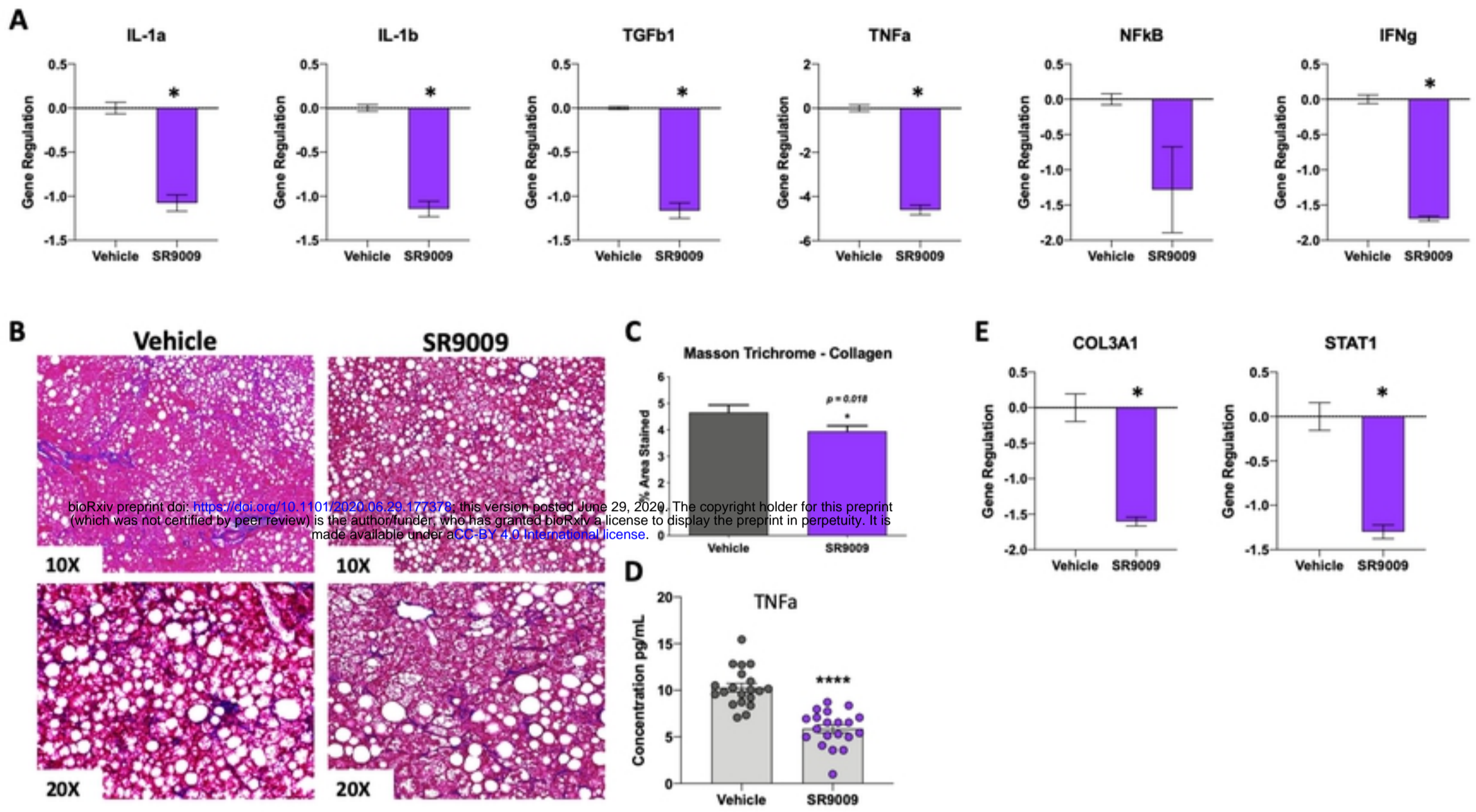


Figure 4